

Sensitivity-Based Discrete Coordinate-Descent for Volt/VAr Control in Distribution Networks

Rabih A. Jabr, *Fellow, IEEE*, and Izudin Džafić, *Senior Member, IEEE*

Abstract—The discrete coordinate-descent algorithm is a practical approach that is currently used in centralized Volt/VAr Control (VVC) implementations, mainly due to its good performance and speed for real-time applications. Its viability is however challenged by the increasing number of distributed generation that contribute to the VVC solution, in addition to the conventional transformer taps and switched capacitors. This paper presents the exact computation of sensitivity factors that speed up the discrete coordinate-descent implementation, by significantly reducing the number of forward/backward substitutions in the current injection power flow method; the speed up is achieved without affecting the control setting quality of the original implementation. The optimality of the discrete coordinate-descent solutions is investigated by computing the gaps relative to mixed-integer linear programming set-points, derived from a polyhedral reformulation of the VVC problem. The sensitivity-based discrete coordinate-descent algorithm is tested starting from two initial points, the default one given by the current control set-points, and a continuous solution obtained from a linear approximation of the VVC problem. Numerical results on networks with up to 3145 nodes show that the sensitivity-based approach significantly improves the runtime of the discrete coordinate-descent algorithm, and that the linear programming initialization leads to VVC solutions with gaps relative to the mixed-integer set-points that are less than 0.5%.

Index Terms—Centralized control, distributed power generation, load flow control, power system simulation, reactive power control, voltage control.

NOMENCLATURE

\underline{a}	A complex-valued quantity, indicated by an underline.
a^{re}, a^{im}	Real and imaginary parts of \underline{a} .
a	Magnitude of \underline{a} .
θ_i	Angle of \underline{V}_i .
BR	Set of all branches.
CAP	Set of nodes having switched capacitors connected to them.
C_I	Penalty coefficient for branch current magnitude violations.
C_V	Penalty coefficient for voltage magnitude violations.

DG	Set of nodes having distributed generation connected to them.
\underline{I}_{ci}	Complex compensation current at node i .
I_{ij}	Current magnitude in branch ij .
n	Number of nodes.
nq, nt	Number of capacitor bank settings and transformer tap positions.
P_{Di}, Q_{Di}	Real and reactive power demand at node i .
P_{Gi}, Q_{Gi}	Real and reactive power generation at node i .
P_i, Q_i	Real and reactive power injection at node i .
Q_{0i}	Nominal Reactive power generation (at 1 pu voltage) by the switched capacitor at node i , chosen from the set $\{Q_{0i}^{(1)}, \dots, Q_{0i}^{(nq)}\}$.
Q_{Ci}	Reactive power generation by the switched capacitor at node i .
t_{ij}	Tap of the transformer in branch ij , chosen from the set $\{t_{ij}^{(1)}, \dots, t_{ij}^{(nt)}\}$.
TR	Set of tap-changing transformer branches.
$\underline{V}, \underline{I}$	Nodal voltage and injection current complex vectors.
$\underline{V}_i, \underline{I}_i$	Nodal voltage and injection current complex values at node i .
V_{slack}	Voltage magnitude at the slack node.
\underline{y}_{ij}	Series admittance of branch ij .
\underline{Y}	Nodal equations coefficient matrix.
\underline{Y}_{ij}^B	Element ij of the bus admittance matrix.
z^{\min}, z^{\max}	Minimum and maximum values of a real-valued quantity z .

I. INTRODUCTION

VOLT/VAr control (VVC) is one of the main functions in the distribution management systems of smart grids; it is integrated into supervisory control and data acquisition (SCADA), which provides real-time input in terms of network configuration and measurements, and real-time output in terms of control actions [1]. Traditional VVC operates on the transformer tap positions and the switchable shunt capacitors with the main goal of removing voltage violations; other secondary objectives include power loss reduction and energy conservation. The increasing levels of distributed generation (DG) in modern distribution networks is known to create voltage violations and thus presents additional challenge to traditional VVC implementations [2], [3]. This paper studies the integration of DG VAr control in centralized VVC, based on the practically

Manuscript received June 18, 2015; revised October 03, 2015; accepted December 22, 2015. Date of publication January 08, 2016; date of current version October 18, 2016. Paper no. TPWRS-00871-2015.

R. A. Jabr is with the Department of Electrical & Computer Engineering, American University of Beirut, Riad El-Solh/Beirut 1107 2020, Lebanon (e-mail: rabih.jabr@aub.edu.lb).

I. Džafić is with the International University of Sarajevo, Hrasnička cesta 15, 71210 Sarajevo, Bosnia (e-mail: idzafic@iee.org).

Digital Object Identifier 10.1109/TPWRS.2015.2512103

accepted discrete coordinate-descent algorithm [1], [4]; it investigates the optimality of the discrete coordinate-descent solutions and proposes exact sensitivity coefficients that serve to speed up the VVC algorithm with DG VAR control.

Practical VVC algorithms are either rule-based or network-based [1]. As their name suggests, rule-based algorithms operate using a predefined set of rules, which are derived based on experience, in addition to limited real-time measurements [5] or dynamically changing system conditions [6]. Although rule-based algorithms are simple to implement, they cannot guarantee good solutions under various operating conditions. Network-based methods make use of a mathematical representation of the distribution network; such a representation requires an estimation of loads [7], which is carried out using real-time measurements together with load curves and automated meter readings. The network-based methods employ mathematical optimization techniques to compute the optimal control set-points of transformer taps, switched capacitors, and DG VAR output in a centralized manner. From a mathematical optimization perspective, network-based VVC is an NP-hard problem involving discrete and continuous variables together with nonlinear constraints [8]. Recently applied methods consider mixed-integer linear programming (MILP) [9] and mixed-integer conic programming [10], [11] formulations; although such techniques are capable of yielding globally optimal solutions for radial network configurations, their numerical performance does not scale well on large networks. Other optimization techniques consider meta-heuristics such as genetic algorithms [12], or hybridizations combining gradient search and meta-heuristics [13]. In practice, the computational performance of mixed-integer optimization and meta-heuristics is not commensurate with the real-time computing requirements on large-scale networks; such techniques have been primarily proposed to solve the off-line setting control problem [2], [10]–[13].

For real-time centralized VVC, the Siemens Energy and Automation research team was the first to propose the discrete coordinate-descent (DCD) algorithm as a viable network-based method [4]; practical experience with this method has shown that it yields good enough solutions with adequate speed for real-time applications. Although the algorithm description in [4] does not explicitly account for DG VAR output, this can be straightforwardly accounted for in the DCD algorithm by discretizing its VAR output range; such a discretization however has an adverse impact on the performance of the algorithm as it necessitates a large increase in the number of power flow solutions. This paper proposes a sensitivity-based technique that significantly improves the runtime of the DCD algorithm, without compromising the quality of the original solution described in [4]. In addition, it presents the first study that characterizes the quality of the DCD-VVC solution through a gap that is computed relative to MILP set-points; the MILP solution is based on mixed-integer conic programming and polyhedral reformulations [10]. In fact, the results show that when DCD is initiated from a rounded linear programming solution, it yields control settings with a gap less than 0.5%. Related research on expert systems for reactive power optimization/voltage control in

transmission networks was reported in [14]–[16]; in particular, [15] describes a practically applied scheme that distinguishes between corrective rescheduling and loss minimization. Unlike [14]–[16], the current approach builds on the DCD method that operates on an objective function combining both corrective rescheduling and loss minimization. The proposed sensitivity-based technique requires computing the sensitivity of the real/imaginary voltage components to each of the control variables; these are calculated using a new exact model in Section V, which is different than the linearized decoupled reactive power model used in [14]–[16]. The linearized reactive model is fundamentally based on the fast-decoupled load flow formulation, and it is typically not applicable in distribution networks due to high R/X ratio. The proposed voltage sensitivity coefficients are also more accurate than the ones proposed in [17] specifically for coordinating local voltage controllers in the load flow problem. In particular, the equations in [17] involve approximations on the effect of local controllers on bus voltages that are not directly targeted by the controllers through set-point specifications.

The rest of this paper is organized as follows. Section II gives a mathematical optimization statement of the VVC problem; the network component models are the same as those recently used to solve the distribution power flow problem with local controllers [17]. The original DCD algorithm and the proposed sensitivity-based variant are described in Sections III and IV, respectively. Section V presents the derivations for the voltage sensitivity, that are central to implementing the proposed approach. Numerical simulations are given in Section VI and the paper is concluded in Section VII. The Appendix presents the mixed-integer polyhedral reformulation of the network-based VVC problem. To simplify the presentation, the application of the approach is detailed using the positive sequence representation of the network; this makes it more suited to European distribution networks. However, the methodology is also applicable to the three-phase unsymmetrical representation of a network with unbalanced loading; such a representation is typical of US distribution networks.

II. VOLT/VAR CONTROL

Consider a distribution network having n nodes, with the first one being the slack power injection node. The network nodal admittance matrix \underline{Y}^B accounts for transformers with off-nominal tap positions (1) (see Fig. 1) and switched capacitor banks (2). The injection currents are related to the node voltages by the nodal equations in (3), in which the first row of the \underline{Y} matrix fixes the voltage at node 1 to the slack voltage magnitude. The nodal current injections (6) account for the real/reactive load demand together with any contribution from DG (7).

$$\underline{Y}_{\text{TR}(i \rightarrow j)} = \begin{bmatrix} t_{ij}^2 \underline{y}_{ij} & -t_{ij} \underline{y}_{ij} \\ -t_{ij} \underline{y}_{ij} & \underline{y}_{ij} \end{bmatrix} \quad (1)$$

$$\underline{Y}_{C(i)} = jQ_{0i} \quad (2)$$

$$\underline{YV} = \underline{I} \quad (3)$$

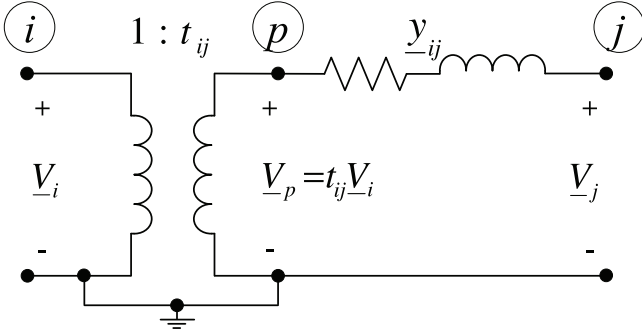


Fig. 1. Tap-changing transformer.

$$\underline{Y} = \begin{bmatrix} 1 & \dots & 0 & \dots & 0 \\ \underline{Y}_{21}^B & \dots & \underline{Y}_{2j}^B & \dots & \underline{Y}_{2n}^B \\ \vdots & \vdots & \vdots & \vdots & \vdots \\ \underline{Y}_{i1}^B & \dots & \underline{Y}_{ij}^B & \dots & \underline{Y}_{in}^B \\ \vdots & \vdots & \vdots & \vdots & \vdots \\ \underline{Y}_{n1}^B & \dots & \underline{Y}_{nj}^B & \dots & \underline{Y}_{nn}^B \end{bmatrix} \quad (4)$$

$$\underline{V} = \begin{bmatrix} \underline{V}_1 \\ \vdots \\ \underline{V}_j \\ \vdots \\ \underline{V}_n \end{bmatrix}; \quad \underline{I} = \begin{bmatrix} V_{\text{slack}} \\ \underline{I}_2 \\ \vdots \\ \underline{I}_i \\ \vdots \\ \underline{I}_n \end{bmatrix} \quad (5)$$

$$\underline{I}_i = \frac{P_i - jQ_i}{\underline{V}_i^*}, \quad i = 2, \dots, n \quad (6)$$

$$P_i = P_{Gi} - P_{Di} \quad (7)$$

$$Q_i = Q_{Gi} - Q_{Di}, \quad i = 2, \dots, n$$

The main aim of VVC is to remove voltage violations, with a secondary objective such as loss minimization. Mathematically, it can be written as an optimization problem whose objective is to minimize the network losses (8) while keeping voltage magnitudes (9) and branch current magnitudes (10) within their prescribed limits. The control variables in the VVC problem are the transformer taps, the capacitor bank settings, and the reactive power contribution from DG. The transformer taps vary in discrete steps (11), with $t_{ij}^{(k)} < t_{ij}^{(k+1)}$. The reactive power injection by capacitor banks is proportional to the square of the nodal voltage, and its nominal value at 1 per-unit voltage also varies in discrete quantities (12), with $Q_{0i}^{(k)} < Q_{0i}^{(k+1)}$. The DG reactive power (13) varies as a continuous variable between its upper and lower limits. The formal statement of the VVC problem is given by (8)–(13), with the nodal voltages and current injections implicitly related by (3)–(7):

$$\min \sum_{i=1}^n \sum_{j=1}^n V_i^{re} Y_{ij}^{re} V_j^{re} + \sum_{i=1}^n \sum_{j=1}^n V_i^{im} Y_{ij}^{re} V_j^{im} \quad (8)$$

subject to:

$$V_i^{\min} \leq V_i \leq V_i^{\max}, \quad i = 1, \dots, n \quad (9)$$

$$I_{ij} \leq I_{ij}^{\max}, \quad ij \in \text{BR} \quad (10)$$

$$t_{ij} \in \{t_{ij}^{(1)}, t_{ij}^{(2)}, \dots, t_{ij}^{(nt)}\}, \quad ij \in \text{TR} \quad (11)$$

$$Q_{Ci} = Q_{0i} V_i^2$$

$$Q_{0i} = \{Q_{0i}^{(1)}, Q_{0i}^{(2)}, \dots, Q_{0i}^{(nq)}\}, \quad i \in \text{CAP} \quad (12)$$

$$Q_{Gi}^{\min} \leq Q_{Gi} \leq Q_{Gi}^{\max}, \quad i \in \text{DG} \quad (13)$$

where:

$$V_i^2 = (V_i^{re})^2 + (V_i^{im})^2 \quad (14)$$

$$I_{ij}^2 = (y_{ij}^{im} (V_i^{re} - V_j^{re}) + y_{ij}^{re} (V_i^{im} - V_j^{im}))^2 + (y_{ij}^{im} (V_i^{im} - V_j^{im}) - y_{ij}^{re} (V_i^{re} - V_j^{re}))^2 \quad (15)$$

III. DISCRETE COORDINATE-DESCENT ALGORITHM

The DCD algorithm is an industry standard for practical VVC implementations [1]. The approach operates on an objective function (16) that penalizes any operational constraint violations, such as voltage and branch current magnitude limits. The algorithm is referred to as a coordinate-descent algorithm because only one variable is updated at each iteration, and it is called discrete because any control variable update is taken in a discrete step. In essence, each iteration requires computing the objective function for all search directions of the control variables; for instance the search directions for a transformer tap which is strictly within limits are: one step up and one step down. Search directions are similarly defined for capacitor bank settings and reactive power from DG, whose operating range is discretized. Rules for choosing the set of search directions in radial distribution networks and for specific objective functions and load representations have been discussed in [4]. The search direction that gives the greatest decrease in objective function is chosen, and the corresponding control variable is then moved in this direction. The iterations of the DCD algorithm continue until there is no search direction that gives an improvement in the objective function value.

$$f = \sum_{i=1}^n \sum_{j=1}^n V_i^{re} Y_{ij}^{re} V_j^{re} + \sum_{i=1}^n \sum_{j=1}^n V_i^{im} Y_{ij}^{re} V_j^{im} + C_V \sum_{i=1}^n \max(0, V_i - V_i^{\max}) + C_V \sum_{i=1}^n \max(0, V_i^{\min} - V_i) + C_I \sum_{ij \in \text{BR}} \max(0, I_{ij} - I_{ij}^{\max}) \quad (16)$$

Reference [4] argues that in order not to add terms of different nature (power loss, voltage violations, current violations) in the same objective function (16), the different terms can be normalized to the same units using the concept of violated power. This is achieved by multiplying the voltage violation by the rated current flowing through the bus in addition to a penalty factor, and the current violation by the rated bus voltage in addition to a penalty factor. The result is that the objective function would minimize the violated power. In practice, the operator can choose different penalty coefficients to reflect different priorities in violations.

The computation of the objective function for each setting of the control variables requires the solution of a power flow

problem. The current injection method [17] is used to solve the power flow; in this method, the injection currents (6) are iteratively updated to correspond to the most recent estimate of nodal voltages, and the nodal voltages are then recomputed using (3). The solution for voltages is obtained using sparse triangular factorization and forward/backward substitution. The power flow problem is solved when the voltages and currents in (3) also satisfy (17):

$$|\underline{V}_i \underline{I}_i^* - (P_i + jQ_i)| \leq \varepsilon, \quad i = 2, \dots, n \quad (17)$$

To have an efficient DCD implementation, the \underline{Y} matrix is factorized only once, and any changes in the tap positions or control settings of the switched capacitor banks are handled using the compensation technique [18]. Specifically, if the \underline{Y} matrix has been formed with the transformer between nodes i and j having the tap t_{ij}^{old} , and the tap position is moved to a new value t_{ij} , then the injection currents at nodes i and j become:

$$\underline{I}'_i = \underline{I}_i + \left[(t_{ij}^{\text{old}})^2 - (t_{ij})^2 \right] \underline{y}_{ij} \underline{V}_i - [t_{ij}^{\text{old}} - t_{ij}] \underline{y}_{ij} \underline{V}_j \quad (18)$$

$$\underline{I}'_j = \underline{I}_j - [t_{ij}^{\text{old}} - t_{ij}] \underline{y}_{ij} \underline{V}_i \quad (19)$$

Similarly, if the \underline{Y} matrix has been initially formed with the capacitor at node i fixed at the set-point Q_{0i}^{old} , and this set-point is moved to the new value Q_{0i} , then the injection current at node i includes a compensation term and becomes:

$$\underline{I}'_i = \underline{I}_i + j [Q_{0i}^{\text{old}} - Q_{0i}] \underline{V}_i \quad (20)$$

For DG connected at node i , the compensation current at this node is simply:

$$\underline{I}_{ci} = \frac{P_{Gi} - jQ_{Gi}}{\underline{V}_i^*} \quad (21)$$

The discrete coordinate-descent algorithm is summarized in the following steps:

- Step 1: Initialize the setting of transformer taps, switched capacitor banks, and reactive power from distributed generation. Set the coordinate-descent iteration counter to 1.
- Step 2: Form the nodal equations matrix \underline{Y} that accounts for the initial settings of transformer taps and switched capacitor banks. Factorize \underline{Y} using LU decomposition: $\underline{Y} = \underline{Y}_L \underline{Y}_U$. The columns of \underline{Y} are ordered for factorization sparsity.
- Step 3: Compute the base-case power flow using the current injection method [17], and calculate the Initial Objective Function (IOF).
- Step 4: Determine the Initial Search Directions, with indices: $\text{SD} = 1, \dots, \text{NSD}$. For each control variable which is neither at the lower limit nor at the upper limit of its control range, its search directions are one step up and one step down. For each control variable at the lower limit of its control range, the search direction is one step up; for each control variable at its upper limit, the search direction is one step down. Initialize $\text{SD} = 1$, and set the index of the Best Search Direction to zero: $\text{BSD} = 0$.

- Step 5: Move the control variable in the direction given by SD. Use the compensation technique [18] to compute the power flow solution and calculate the Current Objective Function (COF). Restore the control variable to its initial value.
- Step 6: If $\text{COF} < \text{IOF}$, then set $\text{IOF} = \text{COF}$ and $\text{BSD} = \text{SD}$, else keep them at their current values.
- Step 7: If $\text{SD} < \text{NSD}$, increment SD by 1 and go to Step 5, else continue to Step-8.
- Step 8: If $\text{BSD} = 0$, end the search (the optimization is complete), else move the control variable in the direction given by BSD, increase the coordinate-descent iteration counter by 1, and go to Step-4.

IV. SENSITIVITY-BASED DISCRETE COORDINATE-DESCENT ALGORITHM

The discrete coordinate-descent algorithm can be made more efficient by computing the sensitivity of the objective function (16) to each of the control variables $(\partial f)/(\partial x)$, and then deciding on the search direction for the variable. For example, if a transformer tap is strictly within limits and its $(\partial f)/(\partial x) > 0$, then the search direction for this variable is one step down; this translates into solving one power flow solution instead of two that correspond to one step up and one step down. The sensitivity based discrete coordinate-descent algorithm has the potential to reduce the number of power flow solutions and consequently speed up the solution process; it requires simply replacing Step-4 in the above algorithm by the following:

Step-4: Determine the Initial Search Directions, with indices: $\text{SD} = 1, \dots, \text{NSD}$. Compute the sensitivity of the objective function $(\partial f)/(\partial x)$ to each of the control variables. For each control variable with a positive sensitivity factor, its search direction is one step down provided the variable itself is not at the lower control limit. Similarly, for each control variable with a negative sensitivity factor, its search direction is one step up provided the variable itself is not at the upper control limit. Initialize $\text{SD} = 1$, and set the index of the Best Search Direction to zero: $\text{BSD} = 0$.

The sensitivity of the objective function with respect to a control variable (22) is computed by applying the chain-rule for derivatives to (16); $h_V(V_i)$ and $h_I(I_{ij})$ are indicator functions given by (23) and (24), t'_{ij} is the transformer tap only for branches that do contain a transformer (25), and $C(x)$ is non-zero only when the control variable is a transformer tap (26). The computation of the sensitivity coefficient (22) requires the values for $(\partial V_i^{\text{re}})/(\partial x)$ and $(\partial V_i^{\text{im}})/(\partial x)$ at all nodes; these values are computed in the next section.

$$\begin{aligned} \frac{\partial f}{\partial x} = & 2 \sum_{i=1}^n \sum_{j=1}^n \frac{\partial V_i^{\text{re}}}{\partial x} Y_{ij}^{\text{re}} V_j^{\text{re}} \\ & + 2 \sum_{i=1}^n \sum_{j=1}^n \frac{\partial V_i^{\text{im}}}{\partial x} Y_{ij}^{\text{re}} V_j^{\text{im}} \\ & + C_V \sum_{i=1}^n h_V(V_i) \frac{V_i^{\text{re}}}{V_i} \frac{\partial V_i^{\text{re}}}{\partial x} \\ & + C_V \sum_{i=1}^n h_V(V_i) \frac{V_i^{\text{im}}}{V_i} \frac{\partial V_i^{\text{im}}}{\partial x} \end{aligned}$$

$$\begin{aligned}
& + C_I \sum_{ij \in \text{BR}} h_I(I_{ij}) \frac{t'_{ij} (t'_{ij} V_i^{re} - V_j^{re}) y_{ij}^2}{I_{ij}} \frac{\partial V_i^{re}}{\partial x} \\
& + C_I \sum_{ij \in \text{BR}} h_I(I_{ij}) \frac{(V_j^{re} - t'_{ij} V_i^{re}) y_{ij}^2}{I_{ij}} \frac{\partial V_j^{re}}{\partial x} \\
& + C_I \sum_{ij \in \text{BR}} h_I(I_{ij}) \frac{t'_{ij} (t'_{ij} V_i^{im} - V_j^{im}) y_{ij}^2}{I_{ij}} \frac{\partial V_i^{im}}{\partial x} \\
& + C_I \sum_{ij \in \text{BR}} h_I(I_{ij}) \frac{(V_j^{im} - t'_{ij} V_i^{im}) y_{ij}^2}{I_{ij}} \frac{\partial V_j^{im}}{\partial x} \\
& + C(x)
\end{aligned} \tag{22}$$

$$h_V(V_i) = \begin{cases} 1, & V_i > V_i^{\max} \\ -1, & V_i < V_i^{\min} \\ 0, & V_i^{\min} \leq V_i \leq V_i^{\max} \end{cases} \tag{23}$$

$$h_I(I_{ij}) = \begin{cases} 1, & I_{ij} > I_{ij}^{\max} \\ 0, & I_{ij} \leq I_{ij}^{\max} \end{cases} \tag{24}$$

$$t'_{ij} = \begin{cases} t_{ij}, & ij \in \text{TR} \\ 1, & ij \notin \text{TR} \end{cases} \tag{25}$$

$$C(x) = 0, \quad x \neq t_{ij}$$

$$\begin{aligned}
C(t_{ij}) &= 2y_{ij}^{re} (t_{ij} V_i^2 - V_i^{re} V_j^{re} - V_i^{im} V_j^{im}) \\
&\quad - \frac{h_I(I_{ij}) y_{ij}^2 (V_i^{re} V_j^{re} + V_i^{im} V_j^{im} - t_{ij} V_i^2)}{I_{ij}}
\end{aligned} \tag{26}$$

V. VOLTAGE SENSITIVITY COMPUTATION

To compute $(\partial V_i^{re})/(\partial x)$ and $(\partial V_i^{im})/(\partial x)$ for $i = 1, \dots, n$, write the nodal equations in terms of the real and imaginary components of nodal voltages, injection currents, and bus admittance values:

$$\begin{bmatrix} Y^{re} & -Y^{im} \\ Y^{im} & Y^{re} \end{bmatrix} \begin{bmatrix} V^{re} \\ V^{im} \end{bmatrix} = \begin{bmatrix} I^{re} \\ I^{im} \end{bmatrix} \tag{27}$$

$$Y^{re} = \begin{bmatrix} 1 & \cdots & 0 & \cdots & 0 \\ Y_{21}^{re} & \cdots & Y_{2j}^{re} & \cdots & Y_{2n}^{re} \\ \vdots & & \vdots & & \vdots \\ Y_{i1}^{re} & \cdots & Y_{ij}^{re} & \cdots & Y_{in}^{re} \\ \vdots & & \vdots & & \vdots \\ Y_{n1}^{re} & \cdots & Y_{nj}^{re} & \cdots & Y_{nn}^{re} \end{bmatrix} \tag{28}$$

$$Y^{im} = \begin{bmatrix} 0 & \cdots & 0 & \cdots & 0 \\ Y_{21}^{im} & \cdots & Y_{2j}^{im} & \cdots & Y_{2n}^{im} \\ \vdots & & \vdots & & \vdots \\ Y_{i1}^{im} & \cdots & Y_{ij}^{im} & \cdots & Y_{in}^{im} \\ \vdots & & \vdots & & \vdots \\ Y_{n1}^{im} & \cdots & Y_{nj}^{im} & \cdots & Y_{nn}^{im} \end{bmatrix} \tag{29}$$

$$V^{re} = \begin{bmatrix} V_1^{re} \\ \vdots \\ V_j^{re} \\ \vdots \\ V_n^{re} \end{bmatrix}; \quad V^{im} = \begin{bmatrix} V_1^{im} \\ \vdots \\ V_j^{im} \\ \vdots \\ V_n^{im} \end{bmatrix} \tag{30}$$

$$I^{re} = \begin{bmatrix} V_{\text{slack}} \\ I_2^{re} \\ \vdots \\ I_i^{re} \\ \vdots \\ I_n^{re} \end{bmatrix}; \quad I^{im} = \begin{bmatrix} 0 \\ I_2^{im} \\ \vdots \\ I_i^{im} \\ \vdots \\ I_n^{im} \end{bmatrix} \tag{31}$$

$$\begin{aligned}
I_i^{re} &= \frac{P_i V_i^{re} + Q_i V_i^{im}}{V_i^2} \\
I_i^{im} &= \frac{P_i V_i^{im} - Q_i V_i^{re}}{V_i^2}, \quad i = 2, \dots, n
\end{aligned} \tag{32}$$

Taking the derivative of each of the nodal equations in (27) with respect to an arbitrary control variable x gives the system of sensitivity equations in (33). The $\underline{Y}_D^{(\bullet,*)}$ sub-matrices in (33) are diagonal matrices; their elements (34)–(37) are computed from the expressions for the real/imaginary injection currents (32) and the chain-rule for derivatives ($i = 2, \dots, n$). The coefficient matrix in (33) is constant at a given iteration; it is ordered for sparsity and factored so that forward/backward substitution can be utilized to efficiently compute the voltage sensitivity with respect to any control variable. The right-hand-side vector in (33) contains the sensitivity of the real/imaginary compensation currents to this control variable. The real/imaginary voltage sensitivity and the corresponding compensation current sensitivity vectors are presented in Subsection V.A for transformer taps, in Subsection V.B for switched capacitor bank settings, and in Subsection V.C for DG reactive power output.

$$\begin{bmatrix} Y^{re} - Y_D^{(re,re)} & -Y^{im} - Y_D^{(re,im)} \\ Y^{im} - Y_D^{(im,re)} & Y^{re} - Y_D^{(im,im)} \end{bmatrix} \begin{bmatrix} \frac{\partial V^{re}}{\partial x} \\ \frac{\partial V^{im}}{\partial x} \end{bmatrix} = \begin{bmatrix} \frac{\partial I^{re}}{\partial x} \\ \frac{\partial I^{im}}{\partial x} \end{bmatrix} \tag{33}$$

$$Y_{Dii}^{(re,re)} = \frac{P_i}{V_i^2} - \frac{2V_i^{re} (P_i V_i^{re} + Q_i V_i^{im})}{V_i^4} \tag{34}$$

$$Y_{Dii}^{(re,im)} = \frac{Q_i}{V_i^2} - \frac{2V_i^{im} (P_i V_i^{re} + Q_i V_i^{im})}{V_i^4} \tag{35}$$

$$Y_{Dii}^{(im,re)} = \frac{-Q_i}{V_i^2} - \frac{2V_i^{re} (P_i V_i^{im} - Q_i V_i^{re})}{V_i^4} \tag{36}$$

$$Y_{Dii}^{(im,im)} = \frac{P_i}{V_i^2} - \frac{2V_i^{im} (P_i V_i^{im} - Q_i V_i^{re})}{V_i^4} \tag{37}$$

A. Transformer Tap

For a control variable $x = t_{ij}$, which is the tap of a transformer between nodes i and j , the real/imaginary voltage sensitivity is given by (38) and the right-hand-side in (33) is given by the vectors in (39); note that all the elements in (39) are zero except for four values. To obtain these nonzero values, express the compensation currents in (18) and (19) in terms of their real

and imaginary components and then take the derivative with respect to t_{ij} ; the resulting expressions are given by (40)–(43).

$$\frac{\partial V^{re}}{\partial t_{ij}} = \begin{bmatrix} \frac{\partial V_1^{re}}{\partial t_{ij}} \\ \vdots \\ \frac{\partial V_j^{re}}{\partial t_{ij}} \\ \vdots \\ \frac{\partial V_n^{re}}{\partial t_{ij}} \end{bmatrix}; \quad \frac{\partial V^{im}}{\partial t_{ij}} = \begin{bmatrix} \frac{\partial V_1^{im}}{\partial t_{ij}} \\ \vdots \\ \frac{\partial V_j^{im}}{\partial t_{ij}} \\ \vdots \\ \frac{\partial V_n^{im}}{\partial t_{ij}} \end{bmatrix} \quad (38)$$

$$\frac{\partial I_c^{re}}{\partial t_{ij}} = \begin{bmatrix} 0 \\ \vdots \\ 0 \\ \frac{\partial I_{ci}^{re}}{\partial t_{ij}} \\ 0 \\ \vdots \\ 0 \\ \frac{\partial I_{cj}^{re}}{\partial t_{ij}} \\ 0 \\ \vdots \end{bmatrix}; \quad \frac{\partial I_c^{im}}{\partial t_{ij}} = \begin{bmatrix} 0 \\ \vdots \\ 0 \\ \frac{\partial I_{ci}^{im}}{\partial t_{ij}} \\ 0 \\ \vdots \\ 0 \\ \frac{\partial I_{cj}^{im}}{\partial t_{ij}} \\ 0 \\ \vdots \end{bmatrix} \quad (39)$$

$$\frac{\partial I_{ci}^{re}}{\partial t_{ij}} = 2t_{ij} (V_i^{im} y_{ij}^{im} - V_i^{re} y_{ij}^{re}) - V_j^{im} y_{ij}^{im} + V_j^{re} y_{ij}^{re} \quad (40)$$

$$\frac{\partial I_{ci}^{im}}{\partial t_{ij}} = -2t_{ij} (V_i^{re} y_{ij}^{im} + V_i^{im} y_{ij}^{re}) + V_j^{im} y_{ij}^{re} + V_j^{re} y_{ij}^{im} \quad (41)$$

$$\frac{\partial I_{cj}^{re}}{\partial t_{ij}} = V_i^{re} y_{ij}^{re} - V_i^{im} y_{ij}^{im} \quad (42)$$

$$\frac{\partial I_{cj}^{im}}{\partial t_{ij}} = V_i^{re} y_{ij}^{im} + V_i^{im} y_{ij}^{re} \quad (43)$$

B. Switched Capacitor Bank Setting

For a control variable $x = Q_{0i}$, which designates the reactive power injection at 1 per-unit voltage, the real/imaginary voltage sensitivity vectors are given by (44) and the right-hand-side vectors (45) contain only two nonzero elements, with their expressions given by (46). These expressions are obtained by writing the compensation current in (20) in terms of its real and imaginary components and then taking the derivative with respect to Q_{0i} .

$$\frac{\partial V^{re}}{\partial Q_{0i}} = \begin{bmatrix} \frac{\partial V_1^{re}}{\partial Q_{0i}} \\ \vdots \\ \frac{\partial V_j^{re}}{\partial Q_{0i}} \\ \vdots \\ \frac{\partial V_n^{re}}{\partial Q_{0i}} \end{bmatrix}; \quad \frac{\partial V^{im}}{\partial Q_{0i}} = \begin{bmatrix} \frac{\partial V_1^{im}}{\partial Q_{0i}} \\ \vdots \\ \frac{\partial V_j^{im}}{\partial Q_{0i}} \\ \vdots \\ \frac{\partial V_n^{im}}{\partial Q_{0i}} \end{bmatrix} \quad (44)$$

$$\frac{\partial I_c^{re}}{\partial Q_{0i}} = \begin{bmatrix} 0 \\ \vdots \\ 0 \\ \frac{\partial I_{ci}^{re}}{\partial Q_{0i}} \\ 0 \\ \vdots \\ 0 \end{bmatrix}; \quad \frac{\partial I_c^{im}}{\partial Q_{0i}} = \begin{bmatrix} 0 \\ \vdots \\ 0 \\ \frac{\partial I_{ci}^{im}}{\partial Q_{0i}} \\ 0 \\ \vdots \\ 0 \end{bmatrix} \quad (45)$$

$$\frac{\partial I_{ci}^{re}}{\partial Q_{0i}} = V_i^{im}, \quad \frac{\partial I_{ci}^{im}}{\partial Q_{0i}} = -V_i^{re} \quad (46)$$

C. Generator Reactive Power Injection

For a control variable equal to the DG VAR generation at node i , i.e., $x = Q_{Gi}$, the voltage sensitivity and right-hand-side vectors are similar to the above case, except for the compensation current in (21) that gives rise to the current injection sensitivity elements given by (49).

$$\frac{\partial V^{re}}{\partial Q_{Gi}} = \begin{bmatrix} \frac{\partial V_1^{re}}{\partial Q_{Gi}} \\ \vdots \\ \frac{\partial V_j^{re}}{\partial Q_{Gi}} \\ \vdots \\ \frac{\partial V_n^{re}}{\partial Q_{Gi}} \end{bmatrix}; \quad \frac{\partial V^{im}}{\partial Q_{Gi}} = \begin{bmatrix} \frac{\partial V_1^{im}}{\partial Q_{Gi}} \\ \vdots \\ \frac{\partial V_j^{im}}{\partial Q_{Gi}} \\ \vdots \\ \frac{\partial V_n^{im}}{\partial Q_{Gi}} \end{bmatrix} \quad (47)$$

$$\frac{\partial I_c^{re}}{\partial Q_{Gi}} = \begin{bmatrix} 0 \\ \vdots \\ 0 \\ \frac{\partial I_{ci}^{re}}{\partial Q_{Gi}} \\ 0 \\ \vdots \end{bmatrix}; \quad \frac{\partial I_c^{im}}{\partial Q_{Gi}} = \begin{bmatrix} 0 \\ \vdots \\ 0 \\ \frac{\partial I_{ci}^{im}}{\partial Q_{Gi}} \\ 0 \\ \vdots \end{bmatrix} \quad (48)$$

$$\frac{\partial I_{ci}^{re}}{\partial Q_{Gi}} = \frac{V_i^{im}}{V_i^2}, \quad \frac{\partial I_{ci}^{im}}{\partial Q_{Gi}} = \frac{-V_i^{re}}{V_i^2} \quad (49)$$

VI. NUMERICAL RESULTS

The VVC algorithms were programmed in Matlab running on an iMAC having a 2.7 GHz quad-core Intel Core i5 processor with 4 MB L3 cache and 8 GB of RAM. The test instances consist of a modified version of a realistic Brazilian distribution system [19] in addition to two test networks with 1463 and 3145 nodes; the complete data sets of the test networks, including their single-line diagrams, can be downloaded from [20]. The main characteristics of the test networks are summarized in Table I, which shows the network configuration (radial/meshed), the loading level expressed in terms of the load multiplying factor (LMF), together with the number of nodes, distributed generation (DG), tap-changing transformers (TR), and switched capacitors (CAP). The networks include tap-changing transformers at the substation and in the middle of some feeders. The number of taps per transformer is normally 33 ($nt = 33$), the number of settings per switched capacitor is chosen to be 5 ($nq = 5$), and the resolution for DG VAR output is 10^{-3} pu. A scaling penalty factor of 100 is used for all constraint violations. Three methods are compared:

- The mixed-integer conic model described in the Appendix and based on [10]; this model is solved via the CPLEX mixed-integer linear programming (MILP) solver after all conic constraints are replaced by tight polyhedral approximations. The default MILP relative optimality gap tolerance is 0.01%.
- The discrete coordinate-descent (DCD) method described in Section III; this method is basically an implementation of Roytelman's algorithm [4] for the formulation (8)–(13) and is indicated in the results by the letters RO.

TABLE I
SUMMARY OF TEST NETWORKS

Name	Config.	LMF	Nodes	DG	TR	CAP
B_R	Radial	1.00	160	7	6	2
B_M	Meshed	1.00	159	7	6	2
1k5_L	Meshed	0.33	1463	5	8	8
1k5_M	Meshed	0.50	1463	5	8	8
1k5_H	Meshed	1.00	1463	5	8	8
3k_L	Meshed	0.50	3145	10	15	13
3k_M	Meshed	0.80	3145	10	15	13
3k_H	Meshed	1.00	3145	10	15	13

- The sensitivity-based discrete coordinate-descent method described in Section IV; this method is indicated in the results by the letters SB.

The two variants of DCD, Roytelman's (RO) and the sensitivity-based (SB) method, were tested starting from two initial points:

- The default initial point given by the original control settings in the test files [20].
- The initial point given by first solving the linear programming (LP) relaxation in the Appendix and then rounding the control set-points to their nearest discrete values; with this initial point, the method is referred to as LP+DCD.

Table II shows the percentage loss reduction (LR) due to the VVC solutions from MILP, the DCD with the default initial point, and the LP+DCD. Because the MILP solution ignores cycle constraints, the obtained control set-points were used to run a power flow and obtain the losses; this led to solutions where some of the voltage constraints in meshed networks are slightly violated (total violation < 0.008 pu)—they are marked by an asterisk sign in Table II. All the solutions from DCD and LP+DCD do not have any constraint violations. Columns 3 and 5 in Table II show the loss reduction for DCD and LP+DCD, respectively, and columns 4 and 6 show the corresponding gap relative to the objective function computed from the MILP control settings (GAP); it is clear that LP+DCD gives a better solution with a maximum $GAP < 0.5\%$. The results in Table II do not distinguish between Roytelman's DCD and the sensitivity-based one because both methods give exactly the same solution. The advantage of the sensitivity-based approach appears in Table III, which shows the number of forward/backward (FB) substitutions in the current injection method; the sensitivity-based FB substitutions translate into a reduction relative to Roytelman's method ($100 \times (FB-RO-FB-SB)/FB-RO$) ranging between 46% and 60%; the main coordinate-descent (CD) iterations are however the same for both RO and SB, further ascertaining that the use of sensitivity information to speed up the classical RO-DCD does not alter the adjustments to the control variables. Table IV shows that the reduction in FB substitutions leads to significantly less computation time for the SB approach, and to a speed up factor ($SUF=(RO-[s])/SB-[s])$) ranging between 1.45 and 2.08. The MILP execution time reaches the set limit of 48 h for the largest test instances, with a maximum relative optimality gap of 0.16%.

It is well known that the behavior of local optimization methods, such as [14]–[16] and the DCD, is dependent on the starting point; the proposal to initiate the DCD search from a near-feasible point, which is obtained from a linear program

TABLE II
PERCENTAGE LOSS REDUCTION AND GAP RELATIVE TO MILP (VALUES MARKED WITH * DENOTE SLIGHT VOLTAGE VIOLATIONS)

Name	MILP	DCD		LP+DCD	
	LR [%]	LR [%]	GAP [%]	LR [%]	GAP [%]
B_R	11.92	11.88	0.0478	11.89	0.0315
B_M	13.84	13.37	0.5453	13.78	0.0689
1k5_L	14.42*	12.14	2.5930	14.40	0.0229
1k5_M	14.47*	11.83	2.9948	14.28	0.2117
1k5_H	18.16*	13.67	5.1947	18.07	0.1109
3k_L	11.76	8.81	3.2317	11.53	0.2569
3k_M	15.65*	11.85	4.3097	15.54	0.1393
3k_H	18.76*	14.56	4.9216	18.42	0.4245

TABLE III
NUMBER OF COORDINATE-DESCENT ITERATIONS AND FORWARD/BACKWARD SUBSTITUTIONS WITH ROYTELMAN'S AND THE SENSITIVITY-BASED APPROACH

Name	DCD			LP+DCD		
	CD	FB-RO	FB-SB	CD	FB-RO	FB-SB
B_R	54	10338	5536	5	870	462
B_M	58	10458	5592	2	295	150
1k5_L	85	20451	8427	16	3530	1595
1k5_M	60	17134	7064	12	3496	1632
1k5_H	72	33141	13397	18	7443	3206
3k_L	73	44290	18311	14	8399	3808
3k_M	80	69605	28734	6	4586	2125
3k_H	79	79136	32576	19	18872	8257

TABLE IV
EXECUTION TIME OF MILP AND THE DISCRETE COORDINATE-DESCENT ALGORITHMS

Name	MILP	DCD			LP+DCD		
	Time	RO-[s]	SB-[s]	SUF	RO-[s]	SB-[s]	SUF
B_R	104 s	1.98	1.24	1.60	0.77	0.53	1.45
B_M	122 s	2.02	1.28	1.58	0.70	0.48	1.46
1k5_L	0.9 h	6.79	3.77	1.80	1.75	1.06	1.65
1k5_M	1.0 h	5.73	3.08	1.86	1.68	1.02	1.65
1k5_H	1.7 h	9.87	4.94	2.00	2.73	1.51	1.81
3k_L	48 h	23.54	11.98	1.96	5.03	2.83	1.78
3k_M	48 h	35.46	17.01	2.08	3.09	1.67	1.85
3k_H	48 h	39.81	18.38	2.17	9.97	5.00	1.99

(DCD+LP), promises to solve any voltage problems that are not alleviated by DCD that starts from the current operating point. In the numerical tests, the DCD+LP solution gives lower losses as compared to DCD starting from the current operating point, while both approaches produce solutions that strictly satisfy operational limits under low, medium, and heavy loading.

VII. CONCLUSION

This paper presented a sensitivity-based discrete coordinate-descent algorithm for solving the VVC problem in modern distribution networks; the sensitivity-based approach speeds up the traditional DCD algorithm particularly with DG sources that contribute to reactive power support. An MILP formulation is proposed to validate the quality of the DCD solutions. The numerical results show that the DCD results on distribution networks with up to 3145 nodes have a gap (relative to the MILP set-point objective) within 0.5% when the starting solution is computed from an LP, and a gap within 5% with the default starting solution at the current controller set-points. The DCD

solutions in all test instances are feasible with no voltage violations, thus conforming to the primary objective of VVC.

APPENDIX

The power flow problem in radial networks can be solved using conic programming; it has been recently shown in [10] that this conic formulation can be extended into a mixed-integer formulation that coordinates the control of line switches, switched capacitor banks, and DG reactive power over different time scales. A relaxation of the VVC problem in radial networks can be directly cast as a mixed-integer conic program, by first defining the following variables: $u_i = (V_i^2)/(\sqrt{2})$ for all nodes, $R_{ij} = V_i V_j \cos(\theta_i - \theta_j)$ for all branches, and $T_{ij} = V_i V_j \sin(\theta_i - \theta_j)$ for all branches. The VVC relaxation problem can be therefore formulated as ($N(i)$ denotes the set of nodes connected to node i by a branch):

$$\min \sum_{i=1}^n \sum_{j \in N(i)} \left[\sqrt{2} y_{ij}^{re} u_i - y_{ij}^{re} R_{ij} \right] \quad (50)$$

subject to:

- Power injection constraints at all nodes

$$\sum_{j \in N(i)} \left[\sqrt{2} y_{ij}^{re} u_i - y_{ij}^{re} R_{ij} - y_{ij}^{im} T_{ij} \right] = P_{Gi} - P_{Di} \quad (51)$$

$$\begin{aligned} \sum_{j \in N(i)} \left[-\sqrt{2} y_{ij}^{im} u_i + y_{ij}^{im} R_{ij} - y_{ij}^{re} T_{ij} \right] \\ = Q_{Gi} + Q_{Ci} - Q_{Di} \end{aligned} \quad (52)$$

- Conic constraints for all branches

$$2u_i u_j \geq R_{ij}^2 + T_{ij}^2, \quad R_{ij} \geq 0, \quad T_{ij} = -T_{ji} \quad (53)$$

- Voltage constraints for all nodes

$$\frac{(V_i^{\min})^2}{\sqrt{2}} \leq u_i \leq \frac{(V_i^{\max})^2}{\sqrt{2}}, \quad u_1 = \frac{(V_{\text{slack}})^2}{\sqrt{2}} \quad (54)$$

- Current magnitude constraints for all branches

$$\sqrt{2} y_{ij}^2 (u_i + u_j) - 2 y_{ij}^2 R_{ij} \leq (I_{ij}^{\max})^2 \quad (55)$$

- Constraints for each transformer branch ij (p is an intermediate node, introducing branch pj —see Fig. 1; nodes i and p form a super-node in the power injection constraints [21])

$$\begin{aligned} b_{ij}^{(k)} \left((t_{ij}^{(1)})^2 - (t_{ij}^{(k)})^2 \right) u_i^{\max} \leq u_p - (t_{ij}^{(k)})^2 u_i \\ \leq b_{ij}^{(k)} \left((t_{ij}^{(nt)})^2 - (t_{ij}^{(k)})^2 \right) u_i^{\max} \end{aligned} \quad k = 1, \dots, nt \quad (56)$$

$$\sum_{k=1}^{nt} b_{ij}^{(k)} = nt - 1, \quad b_{ij}^{(k)} \in \{0, 1\} \quad (57)$$

- Constraints for each capacitor bank at node i

$$\begin{aligned} b_i^{(k)} \sqrt{2} \left(Q_{0i}^{(1)} - Q_{0i}^{(k)} \right) u_i^{\max} \leq Q_{Ci} - \sqrt{2} Q_{0i}^{(k)} u_i \\ \leq b_i^{(k)} \sqrt{2} \left(Q_{0i}^{(nq)} - Q_{0i}^{(k)} \right) u_i^{\max} \end{aligned} \quad k = 1, \dots, nq \quad (58)$$

$$\sum_{k=1}^{nq} b_i^{(k)} = nq - 1, \quad b_i^{(k)} \in \{0, 1\} \quad (59)$$

- Reactive power generation by DG at node i

$$Q_{Gi}^{\min} \leq Q_{Gi} \leq Q_{Gi}^{\max} \quad (60)$$

The solution to the relaxation (50)–(60) is valid for the original VVC problem in radial networks provided that the conic constraints in (53) are binding at the optimal solution, a condition which is likely to hold under normal operation. However, even if the conic constraints are binding at optimality, the solution to (50)–(60) will not be generally valid for meshed distribution networks because cycle constraints are not accounted for [21]; if the solution satisfies the cycle constraints then it is indeed a global optimum for the meshed VVC problem, otherwise it serves as a lower bound. In general, even if the conic constraints are not binding or the cycle constraints (in meshed networks) are not satisfied, the mixed-integer objective function value gives a tight lower bound which can be used to gauge the quality of the discrete coordinate-descent solution. The conic constraints in (53) can be tightly approximated by a set of polyhedral constraints [10]; this allows obtaining the solution of the VVC relaxation via MILP, whose solver technology is more developed as compared to mixed-integer conic programming. Additionally if the binary variables in (57) and (59) are treated as continuous, the VVC relaxation can be solved efficiently via linear programming to give a continuous solution of the discrete control variables; these variables can be rounded to their nearest discrete set-points to give a starting point for the discrete coordinate-descent algorithm—c.f. Step-1 in Section III.

REFERENCES

- [1] I. Roytelman, B. K. Wee, R. L. Lugtu, T. M. Kulas, and T. Brossart, "Pilot project to estimate the centralized volt/VAR control effectiveness," *IEEE Trans. Power Syst.*, vol. 13, no. 3, pp. 864–869, Aug. 1998.
- [2] F. A. Viawan and D. Karlsson, "Voltage and reactive power control in systems with synchronous machine-based distributed generation," *IEEE Trans. Power Del.*, vol. 23, no. 2, pp. 1079–1087, Apr. 2008.
- [3] P. M. S. Carvalho, P. F. Correia, and L. A. F. M. Ferreira, "Distributed reactive power generation control for voltage rise mitigation in distribution networks," *IEEE Trans. Power Syst.*, vol. 23, no. 2, pp. 766–772, May 2008.
- [4] I. Roytelman, B. K. Wee, and R. L. Lugtu, "Volt/VAR control algorithm for modern distribution management system," *IEEE Trans. Power Syst.*, vol. 10, no. 3, pp. 1454–1460, Aug. 1995.
- [5] M. E. Baran and M.-Y. Hsu, "Volt/VAR control at distribution substations," *IEEE Trans. Power Syst.*, vol. 14, no. 1, pp. 312–318, Feb. 1999.
- [6] V. Borozan, M. E. Baran, and D. Novosel, "Integrated volt/VAR control in distribution systems," in *Proc. 2001 IEEE Power Eng. Soc. Winter Meeting*, 2001, vol. 3, pp. 1485–1490.
- [7] I. Džafić, M. Gilles, R. A. Jabr, B. C. Pal, and S. Henselmeyer, "Real time estimation of loads in radial and unsymmetrical three-phase distribution networks," *IEEE Trans. Power Syst.*, vol. 28, no. 4, pp. 4839–4848, Nov. 2013.
- [8] R. Baldick and F. F. Wu, "Efficient integer optimization algorithms for optimal coordination of capacitors and regulators," *IEEE Trans. Power Syst.*, vol. 5, no. 3, pp. 805–812, Aug. 1990.
- [9] A. Borghetti, "Using mixed integer programming for the volt/VAR optimization in distribution feeders," *Elect. Power Syst. Res.*, vol. 98, pp. 39–50, May 2013.
- [10] R. A. Jabr, "Minimum loss operation of distribution networks with photovoltaic generation," *IET Renew. Power Gener.*, vol. 8, no. 1, pp. 33–44, Jan. 2014.
- [11] L. H. Macedo, J. F. Franco, M. J. Rider, and R. Romero, "Optimal operation of distribution networks considering energy storage devices," *IEEE Trans. Smart Grid*, vol. 6, no. 6, pp. 2825–2836, Nov. 2015.

- [12] Z. Hu, X. Wang, H. Chen, and G. A. Taylor, "Volt/VAr control in distribution systems using a time-interval based approach," *IEE Proc.-Gener. Transm. Distrib.*, vol. 150, no. 5, pp. 548–554, Sep. 2003.
- [13] A. Mohapatra, P. R. Bijwe, and B. K. Panigrahi, "An efficient hybrid approach for Volt/Var control in distribution systems," *IEEE Trans. Power Del.*, vol. 29, no. 4, pp. 1780–1788, Aug. 2014.
- [14] A. G. Expósito, J. L. M. Ramos, J. L. R. Macías, and Y. C. Salinas, "Sensitivity-based reactive power control for voltage profile improvement," *IEEE Trans. Power Syst.*, vol. 8, no. 3, pp. 937–945, Aug. 1993.
- [15] J. L. M. Ramos, A. G. Expósito, J. C. Cerezo, E. M. Ruiz, and Y. C. Salinas, "A hybrid tool to assist the operator in reactive power/voltage control and optimization," *IEEE Trans. Power Syst.*, vol. 10, no. 2, pp. 760–768, May 1995.
- [16] S. P. Singh, G. S. Raju, and A. K. Gupta, "Sensitivity based expert system for voltage control in power system," *Int. J. Elect. Power Energy Syst.*, vol. 15, no. 3, pp. 131–136, Jun. 1993.
- [17] I. Džafić, R. A. Jabr, E. Halilovic, and B. C. Pal, "A sensitivity approach to model local voltage controllers in distribution networks," *IEEE Trans. Power Syst.*, vol. 29, no. 3, pp. 1419–1428, May 2014.
- [18] W. F. Tinney, "Compensation methods for network solutions by optimally ordered triangular factorization," *IEEE Trans. Power App. Syst.*, vol. PAS-91, no. 1, pp. 123–127, Jan. 1972.
- [19] J. R. S. Mantovani, F. Casari, and R. A. Romero, "Reconfiguração de sistemas de distribuição radiais utilizando o critério de queda de tensão," *SBA: Controle & Automação*, vol. 11, no. 3, pp. 150–159, Dec. 2000.
- [20] VVC Distribution Network Data Sets accessed: Jun. 16, 2015 [Online]. Available: https://dl.dropboxusercontent.com/u/47198710/VVC_DIST_NET.zip
- [21] R. A. Jabr, "Optimal power flow using an extended conic quadratic formulation," *IEEE Trans. Power Syst.*, vol. 23, no. 3, pp. 1000–1008, Aug. 2008.

Rabih Jabr (M'02–SM'09–F'16) was born in Lebanon. He received the B.E. degree in electrical engineering (with high distinction) from the American University of Beirut, Beirut, Lebanon, in 1997 and the Ph.D. degree in electrical engineering from Imperial College London, London, U.K., in 2000.

Currently, he is a Professor in the Department of Electrical and Computer Engineering at the American University of Beirut. His research interests are in mathematical optimization techniques and power system analysis and computing.

Izudin Džafić (M'05–SM'13) received the Ph.D. degree from University of Zagreb, Croatia in 2002.

He is currently an Associate Professor in the Department of Electrical Engineering at the International University of Sarajevo, Bosnia. From 2002 to 2014, he was with Siemens AG, Nuremberg, Germany, where he held the position of the Head of the Department and Chief Product Owner (CPO) for Distribution Network Analysis (DNA) R&D. His research interests include power system modeling, development and application of fast computing to power systems simulations.

Dr. Džafić is a member of the IEEE Power and Energy Society and the IEEE Computer Society.